International Journal of Recent Engineering Science
ISSN: 2349-7157/ https://doi.org/10.14445/23497157/IJRES-V12I4P108

Volume 12 Issue 4, 86-96, Jul-Aug 2025

Original Article

Modeling and Simulation of Reactive and Pressure Swing Distillation Columns for Ethyl Acetate Production using Aspen Plus and MATLAB

Yiga F[1], Okwu K. C[1]

[1]*Department of Chemical/Petrochemical Engineering, Rivers State University, Rivers, Nigeria.*

Corresponding Author：yiga.francis@ust.edu.ng

Received: 18 June 2025 Revised: 24 July 2025 Accepted: 15 August 2025 Published: 30 August 2025

Abstract *- This study develops mathematical models for the esterification of ethanol and acetic acid to produce and separate ethyl acetate from unreacted reactants in a Reactive Distillation Column (RDC). The models describe six discrete column envelopes: reflux drum, rectifying, reactive, feed, stripping, and column base. Four trays (stages 4–7) form the reactive zone, where ethyl acetate and water form alongside unreacted ethanol and acetic acid. The ethyl acetate–ethanol azeotrope forms at the top of the RDC and undergoes separation using Pressure Swing Distillation (PSD). In Aspen Plus, The High-Pressure Column (HPC) operates at 12 bar and 185°C, while the low-pressure column (LPC) runs at 0.5 bar and 45°C. Simulations yield 0.4123 mole ethanol and 0.5877 mole ethyl acetate (ASPEN PLUS) and 0.4356 mole ethanol and 0.5644 mole ethyl acetate (MATLAB) before PSD; values improve to 0.2589 mole ethanol and 0.7411 mole ethyl acetate after PSD. Comparison with literature data (0.2234 mole ethanol, 0.7766 mole ethyl acetate) reveals deviations of 13.74% for ethanol and −4.57% for ethyl acetate. A 10-stage column design improves separation, and optimal feed staging (ethanol at stage 7, acetic acid at stage 4) enhances purity. The results validate PSD's effectiveness and offer a scalable, energy-efficient pathway for high-purity ethyl acetate production.*

Keywords *- Azeotrope, Ethyl acetate-ethanol, Reactive distillation column, Pressure swing distillation.*

1. Introduction

Ethyl acetate ($CH_3COOC_2H_5$) is an important industrial ester widely utilized in various sectors due to its desirable physical and chemical properties: its pleasant odor, low toxicity, high volatility, and excellent solvency. It finds extensive application in paints, adhesives, inks, coatings, pharmaceuticals, and as a flavoring and fragrance agent in the food and cosmetics industries (Calvar et al., 2006; Niu et al., 2022; Singh et al., 2023). In 2023, the global market for ethyl acetate was estimated at USD 5.2 billion and is expected to expand at a Compound Annual Growth Rate (CAGR) of 8.5% through 2028, mainly due to rising demand for environmentally friendly solvents and the expansion of the pharmaceutical and polymer sectors (Mordor Intelligence, 2024; Statista, 2024).

Fischer esterification involves a reversible reaction between ethanol and acetic acid, catalyzed by an acid. Despite the simplicity of the esterification reaction, achieving high yields and purity of ethyl acetate remains challenging due to the chemical equilibrium limitations and the formation of azeotropes between ethanol and ethyl acetate. This azeotrope significantly complicates downstream separation, rendering conventional distillation methods inefficient (Zhang et al., 2021; Gautam et al., 2013). To overcome these challenges, Reactive Distillation (RD) has gained attention as an effective technique that combines reaction and separation within one unit. This approach improves conversion by constantly extracting the products, which drives the equilibrium in favor of product generation. It also minimizes energy usage, reduces capital cost, and simplifies process design by eliminating the need for a separate reactor and distillation unit (Taylor & Krishna, 2020; Wahnschafft et al., 2021).

In the esterification reaction for ethyl acetate production, RD is particularly advantageous because the exothermic nature of the reaction contributes to internal heat integration and efficient separation (Arora et al., 2023).

However, a significant challenge persists: the formation of a pressure-sensitive azeotrope between ethanol and ethyl acetate, which limits product purity even when using RD. This azeotrope exhibits variation with pressure, shifting from lower mole of ethyl acetate formation at 12 bar to a higher mole of ethyl acetate formation at 0.5 bar (Gmehling et al.,

2022; Calvar et al., 2006). This characteristic has led to growing interest in Pressure Swing Distillation (PSD), which employs two distillation columns functioning at varying pressures to break azeotropic mixtures. PSD exploits the volatility differences under varying pressures to disrupt azeotropic behavior and enable efficient product recovery (Zhang et al., 2021; Liu et al., 2023).

Recent literature highlighted several advancements in esterification via RD and PSD. For instance, Niu et al. (2022) investigated RD with energy integration for ethyl acetate synthesis but did not include the pressure-based azeotrope separation technique. Wahnschafft et al. (2021) developed a simulation model using shortcut and rigorous methods for esterification processes, but they did not consider pressure-sensitive systems. Lone and Ahmad (2012) developed a simulation model for ethyl acetate production using Aspen Plus and the RADFRAC module, but pressure-sensitive distillation systems and azeotropic behavior were not considered.

Chern (2019) reviewed various process intensification strategies for ester production using Reactive Distillation (RD) and Pressure-Swing Reactive Distillation (PSRD). While the study emphasized energy savings and operational efficiency, it did not apply PSRD to ethyl acetate systems. Pressure-dependent azeotrope disruption and column integration strategies were not explored for this compound. Kandanapitiya and Gunasekera (2015) developed a batch reactive distillation framework for acetic acid esterification, focusing on conversion efficiency and equilibrium modeling". However, the study did not consider the influence of pressure on azeotropic behavior, limiting its applicability to pressure-sensitive systems like ethyl acetate–ethanol mixtures under varying operating conditions. Lee et al. (2016) "designed a combined reactive distillation–pervaporation for producing ethyl acetate, utilizing membrane separation to eliminate water; however, the use of pressure-swing distillation for managing azeotropes was not explored".

Zhang et al. (2017) "developed a thermally integrated PSD system for ethanol–ethyl acetate separation using Aspen Plus and Dynamics, but reactive distillation coupling with PSD under dynamic operating conditions was not considered".

Arora et al. (2023) proposed a hybrid RD-pervaporation system for butyl acetate production, improving selectivity but failing to address the volatility shifts critical to ethyl acetate-ethanol mixtures. Singh et al. (2023) combined MATLAB and Aspen PLUS for esterification modeling but did not focus on dual-column PSD for azeotrope removal. Clearly, while significant progress has been made, the integration of RD with PSD using hybrid simulation platforms remains underexplored.

In addition, prior works often rely solely on one modeling platform, ASPEN PLUS or MATLAB, each with inherent strengths and limitations. ASPEN PLUS excels in rigorous vapor-liquid equilibrium (VLE) modeling using thermodynamic packages like Non-Random Two-Liquid (NRTL) or UNIQUAC, but offers limited flexibility for custom differential equation solving or dynamic simulation.

In contrast, MATLAB is highly suited for custom kinetic modeling, sensitivity analysis, and numerical solutions of stage-wise material and energy balances but lacks built-in thermodynamic rigor. A combined approach that leverages the strengths of both platforms can provide a more accurate and comprehensive simulation of complex distillation systems (Huang et al., 2019; Singh et al., 2023).

Although numerous studies exist on esterification and distillation methods, comprehensive simulation frameworks that merge reactive distillation with pressure-swing distillation for ethyl acetate production—validated using both ASPEN PLUS and MATLAB—remain scarce. Furthermore, few studies delve into the impact of feed stage optimization, temperature profiling, and pressure conditions on azeotrope elimination and overall purity. The absence of a holistic model limits industrial scalability and control strategies for high-purity ethyl acetate production.

This research fills the identified gap by creating and verifying a detailed simulation model for ethyl acetate production through reactive and pressure swing distillation, employing a combined methodology that integrates ASPEN PLUS with MATLAB.

This hybrid model enables cross-validation, improves simulation accuracy, and enhances understanding of both chemical kinetics and separation dynamics. It demonstrates the capability of PSD to disrupt azeotropic behavior, confirming the viability of the integrated process for high-efficiency and scalable ethyl acetate production.

2. Materials and Methods

2.1. Materials

ASPEN PLUS and MATLAB were employed to simulate the reactive and pressure swing distillation columns and solve custom models.

2.2. Methods

Figure 1 displays a discrete envelope of a reactive distillation column divided into functional sections: reflux drum, rectifying, reactive, feed, stripping, and base to simplify analysis. Each envelope handles specific roles such as reaction, separation, or phase change, enabling targeted mass and energy balances for accurate modeling and process optimization. Figure 2 shows a representative tray of the reactive distillation column.

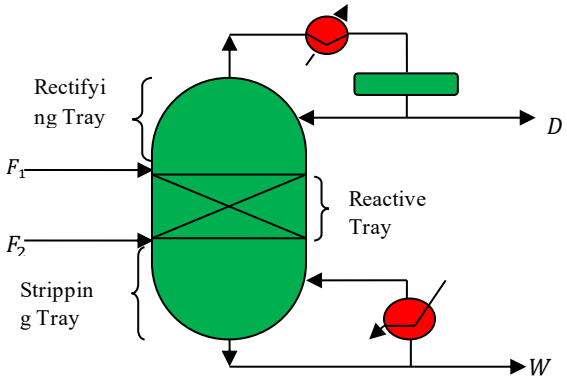

Fig. 1 Hypothetical reactive distillation column

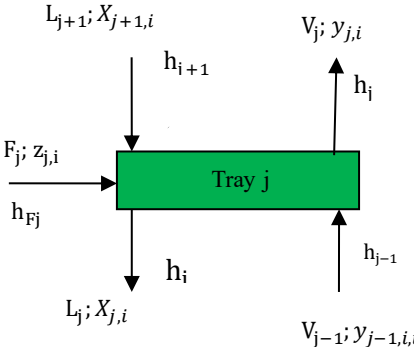

Fig. 2 Representative Tray j

2.2.1. Model Assumptions

- Steady-state operation
- The system is well lagged
- Constant relative volatility
- Constant liquid hold-up
- The reaction occurs in 4 stages (4–7)
- Uniform composition of the reacting mixture
- Six-column envelope

2.2.2. Development of Mathematical Models

Applying the Conservation Principle of Mass and Energy, we have

$$\begin{pmatrix}\text{Rate of material}\\ \text{accumulation}\\ \text{on tray j}\end{pmatrix}=\begin{pmatrix}\text{Rate of material}\\ \text{input}\\ \text{into tray j}\end{pmatrix}-\begin{pmatrix}\text{Rate of material}\\ \text{output}\\ \text{from tray j}\end{pmatrix}\pm\begin{pmatrix}\text{Rate of material}\\ \text{depletion/generation}\\ \text{by chemical reaction on tray j}\end{pmatrix} \quad (1)$$

$$\begin{pmatrix}\text{Rate of energy}\\ \text{accumulation}\\ \text{on tray j}\end{pmatrix}=\begin{pmatrix}\text{Rate of energy}\\ \text{input}\\ \text{into tray j}\end{pmatrix}-\begin{pmatrix}\text{Rate of energy}\\ \text{output}\\ \text{out of tray j}\end{pmatrix}\pm\begin{pmatrix}\text{Rate of energy of}\\ \text{depletion/generation}\\ \text{by chemical reaction on tray j}\end{pmatrix} \quad (2)$$

At steady operation, there is no accumulation of material. Application of equation (1) to tray j gives

Material Balance over Tray j

$$F_j + L_{j+1} + V_{j-1} = L_j + V_j \quad (3)$$

Taking component balance for any species i, from equation (3), we have

$$F_j Z_{j,i} + L_{j+1}x_{j+1,i} + V_{j-1}y_{j-1,i} = L_j x_{j,i} + V_j y_{j,i} + r_{j,i} \quad (4)$$

Phase Equilibrium Relationships

$$y_{j,i} = K_{j,i}x_{j,i} \quad (1 \le j \le Nt,\ 1 \le i \le n) \quad (5)$$

Summations of Mole Fractions

$$\sum_{i=1}^{n} x_{j,i} = 1,\ \sum_{i=1}^{n} y_{j,i} = 1 \quad (6)$$

Combining equations (4) and equation (6), we have

$$F_j Z_{j,i} + L_{j+1}x_{j+1,i} + V_{j-1}K_{j-1,i}x_{j-1,i} = L_j x_{j,i} + V_j K_{j,i}x_{j,i} + r_{j,i} \quad (7)$$

$$K = K_{j-1} = K_j = K_{j+1} \quad (8)$$

$$y_{j,i} = Kx_{j,i} \quad (9)$$

$$F_j Z_{j,i} + L_{j+1}x_{j+1,i} + V_{j-1}Kx_{j-1,i} = L_j x_{j,i} + V_j Kx_{j,i} + r_{j,i} \quad (10)$$

Rectification Envelope

In the rectifying envelope of the column, neither feed is introduced, nor do chemical reactions occur.

$$L_{j+1}x_{j+1,i} + V_{j-1}Kx_{j-1,i} = L_j x_{j,i} + V_j Kx_{j,i} \quad (11)$$

Stripping Envelope

In the stripping envelope of the column, neither feed is introduced, nor chemical reactions occur.

$$L_{j+1}x_{j+1,i} + V_{j-1}Kx_{j-1,i} = L_j x_{j,i} + V_j Kx_{j,i} \quad (12)$$

Feed Tray

$$F_j Z_{j,i} + L_{j+1} x_{j+1,i} + V_{j-1} K x_{j-1,i} = L_j x_{j,i} + V_j K x_{j,i} \quad (13)$$

Reactive Envelope

$$L_{j+1} x_{j+1,i} + V_{j-1} K x_{j-1,i} = L_j x_{j,i} + V_j K x_{j,i} + r_{j,i} \quad (14)$$

Reflux Drum Envelope

$$V_{j-1} K x_{j-1,i} = L_j x_{j,i} + D x_{D,i} \quad (15)$$

Column Base Envelope

$$L_{j+1} x_{j+1,i} = V_j K x_{j,i} + B x_{B,i} \quad (16)$$

Energy Balance over Tray j

At steady operation, there is no accumulation of energy. Application of equation (2) to tray j gives

$$F_j h_{Fj} + L_{j+1} h_{j+1} + V_{j-1} h_{j-1} = L_j h_j + V_j h_j + (-\Delta H_R) r_{ji} \quad (17)$$

$$F_j h_{Fj} + L_{j+1} C_{P_{j+1}} T_{j+1} + V_{j-1} C_{P_{j-1}} T_{j-1} = L_j C_{P_j} T_j + V_j C_{P_j} T_j + (-\Delta H_R) r_{ji} \quad (18)$$

Rectification Envelope

In the rectifying envelope of the column, neither feed is introduced, nor do chemical reactions occur.

$$L_{j+1} C_{P_{j+1}} T_{j+1} + V_{j-1} C_{P_{j-1}} T_{j-1} = L_j C_{P_j} T_j + V_j C_{P_j} T_j \quad (19)$$

Stripping Envelope

In the stripping envelope of the column, neither feed is introduced, nor do chemical reactions occur.

$$L_{j+1} C_{P_{j+1}} T_{j+1} + V_{j-1} C_{P_{j-1}} T_{j-1} = L_j C_{P_j} T_j + V_j C_{P_j} T_j \quad (20)$$

Reactive Envelope

$$L_{j+1} C_{P_{j+1}} T_{j+1} + V_{j-1} C_{P_{j-1}} T_{j-1} = L_j C_{P_j} T_j + V_j C_{P_j} T_j + (-\Delta H_R) r_{ji} \quad (21)$$

Reflux Drum Envelope

$$V_{j-1} C_{P_{j-1}} T_{j-1} = L_j C_{P_j} T_j + D C_{P_D} T_D - Q_{COND} \quad (22)$$

Column Base Envelope

$$L_{j+1} C_{P_{j+1}} T_{j+1} = V_j C_{P_j} T_j + B C_{P_B} T_B + Q_{REB} \quad (23)$$

2.2.3. Kinetics Model

Consider the reversible reaction taking place in the distillation column

$$C_2H_5O + C_2H_4O_2 \leftrightarrow C_4H_8O_2 + H_20 \quad (24)$$

Let $A = C_2H_5O$; $B = C_2H_4O_2$; $C = C_4H_8O_2$; $D = H2O$

The rate of the reaction is given as:

$$(-r_A) = k_1 C_A C_B - k_2 C_C C_D \quad (25)$$

The concentration of any species is written as

$$C_{i,j} = x_{i,j} C_{T,j} \quad (26)$$

$$r_{ji} = \left(\frac{M_j}{V_{Rj}}\right)^2 (k_{1,j} x_{j,A} x_{j,B} - k_{2,j} x_{j,C} x_{j,D} \quad (27)$$

$$\text{But, } C_T = \frac{M_j}{V_{Rj}} \quad (28)$$

2.2.4. Simulation Input Data

Table 1. Feed streams data

Input Parameters	Ethanol	Acetic Acid
Inlet stage	7	4
Temperature (°C)	25	70
Pressure(Bar)	12	12
Flowrate (Kmol/hr)	100	100
Mole fraction	1.0	1.0

Table 2. Column configuration

Parameters	HP Column	LP Column
No of stage	10	10
Reflux ratio	3	2.5
Pressure (Bar)	12	0.5
Reboiler Temperature(°C)	185	45

2.2.4. Simulation with Aspen PLUS

Aspen Plus was used to simulate the production of ethyl acetate through reactive and pressure swing distillation, leveraging its robust capabilities for steady-state modeling of complex chemical processes. The simulation began by selecting the RadFrac model, which was well-suited for combined reaction and separation processes in distillation columns. Primary components—ethanol, acetic acid, ethyl acetate, and water—were specified using the Aspen component library, with the Non-Random Two-Liquid (NRTL) thermodynamic model selected for its demonstrated precision in managing non-ideal systems and azeotropic interactions, especially between ethanol and ethyl acetate. The esterification process involving ethanol and acetic acid was simulated as an equilibrium reaction, occurring exclusively on trays 4 through 7, which correspond to the reactive section of the High-Pressure Column (HPC). Two columns were configured in the simulation: the HPC, operating at 12 bar and 185°C, was responsible for both reaction and initial separation, while the Low-Pressure

Column (LPC), operating at 0.5 bar and 45°C, facilitated azeotrope breaking through Pressure Swing Distillation (PSD). Each column comprised 10 stages, incorporating a condenser and a reboiler. Feed streams of pure ethanol and acetic acid were introduced at trays 7 and 4, respectively, with flow rates, temperatures, and pressures set according to optimized design parameters. The reaction kinetics and separation processes were tightly coupled within the model. ASPEN PLUS simultaneously solved the material balances, energy balances, and phase equilibrium equations across all stages. The software calculated component compositions, conversions, and temperature profiles throughout the columns. The azeotrope formed at the top of the HPC was effectively separated in the LPC due to the shift in volatility under reduced pressure.

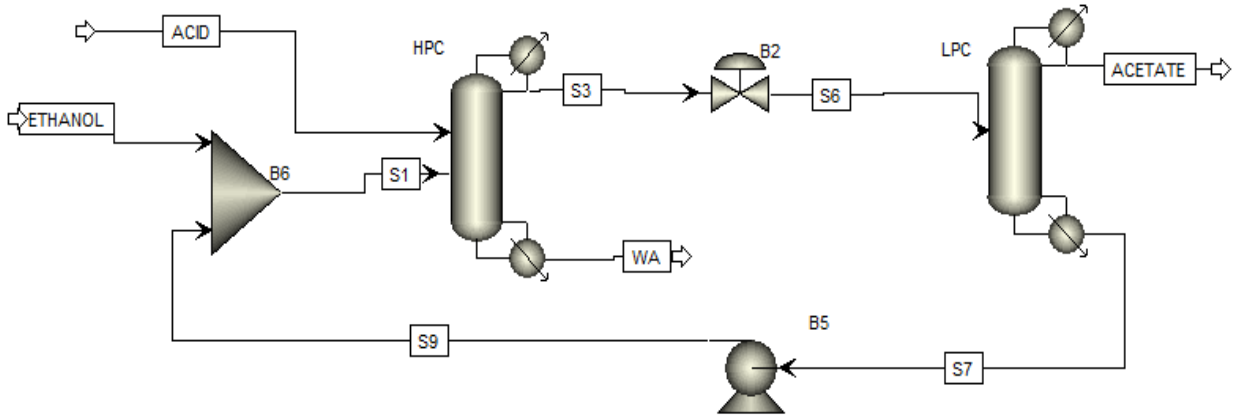

Fig. 3 Flowsheet of Reactive and Pressure Swing Column

3. Results and Discussion

Table 3. Comparison of ASPEN PLUS and MATLAB Stream Composition (HPC)

Component	Aspen PLUS (mole)	MATLAB (mole)
Ethanol	0.4123	0.4356
Ethyl Acetate	0.5877	0.5644

Table 4. Azeotrope Results

Component	Before PSD (Mole)	After PSD (Mole)
Ethanol	0.4123	0.2589
Ethyl Acetate	0.5877	0.7411

Table 5. Simulation validation

Components	ASPEN PLUS (mole)	Literature Data (mole)	% Deviation
Ethanol	0.2589	0.2234	13.74
Ethyl Acetate	0.7411	0.7766	-4.57

Tables 3 to 5 provide a comprehensive evaluation of the modeling and simulation accuracy for ethyl acetate production via reactive and pressure swing distillation using ASPEN PLUS and MATLAB. Table 3 compares stream compositions from the High-Pressure Column (HPC) at 12 bar, where ASPEN PLUS reported 0.5877 mole ethyl acetate and 0.4123 mole ethanol, while MATLAB gave 0.5644 and 0.4356, respectively. The 4% deviation reflected MATLAB's reliance on simplified numerical solvers, whereas ASPEN PLUS used rigorous NRTL thermodynamics, offering higher precision. Table 4 highlights the azeotrope's pressure sensitivity: at 0.5 bar, the azeotrope shifted to 0.7411 mole ethyl acetate and 0.2589 mole ethanol, enabling separation via pressure swing distillation (PSD). This behavior aligned with literature showing azeotrope variation with pressure. Table 5 validated LPC output against literature data (0.7766 ethyl acetate; 0.2234 ethanol), showing acceptable deviations of -4.57% and 13.74% from ASPEN PLUS simulation. [11] The 10-stage design in both columns optimized conversion and purity. Together, these results confirmed the effectiveness of ASPEN PLUS and MATLAB in simulating a scalable, high-efficiency ethyl acetate production process.

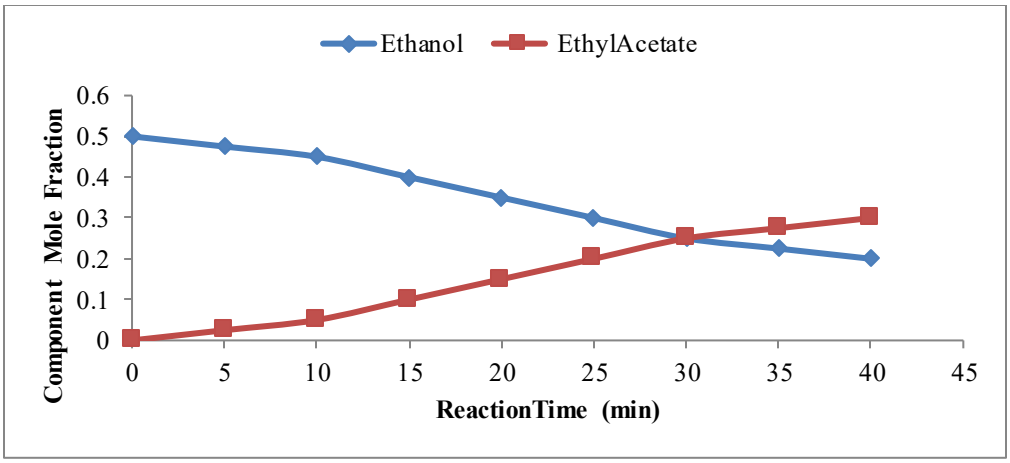

Fig. 4 Component Mole Fraction vs Reaction Time

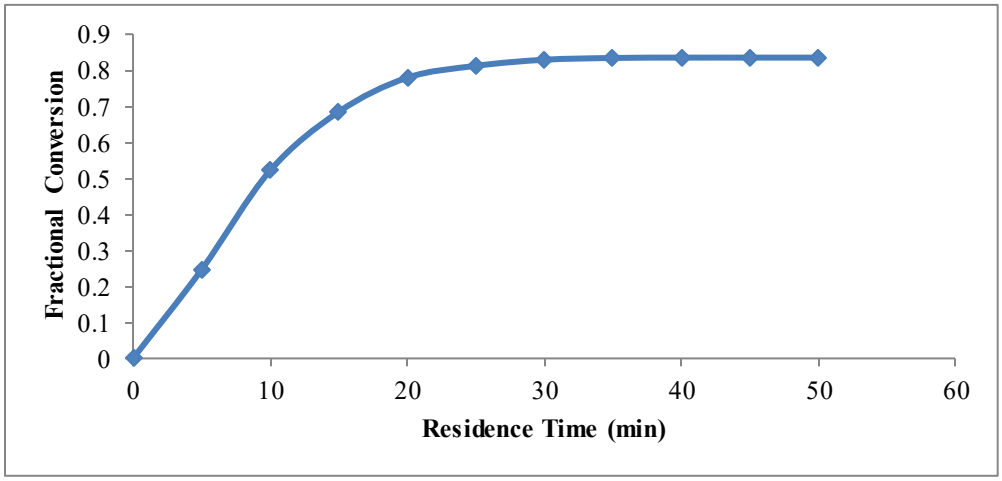

Fig. 5 Fractional Conversion Vs Residence Time

Figure 4 illustrates the dynamic behavior of reactants and products (ethanol and ethyl acetate) concentrations in the high-pressure reactive distillation column over time. Initially, the system contained pure ethanol and acetic acid at equimolar quantities, reacting as the system reached the desired temperature and pressure. As time progressed, the mole fraction of ethanol decreased steadily from 0.5mole to 0.2 mole due to its consumption in the esterification reaction. Simultaneously, ethyl acetate concentration rose from zero moles to 0.3 moles, signifying successful product formation. The curve flattened towards the end, indicating that equilibrium was approached. The profile confirmed that the reaction was favored under the simulated conditions, with efficient conversion achieved within 40 minutes. The consistent rise in ethyl acetate and fall in ethanol validated the effectiveness of continuous removal in reactive distillation, which shifted the equilibrium toward the product side. This behavior reinforced the application of reactive distillation for process intensification, showcasing simultaneous, time-dependent conversion and separation within one unit. It also highlighted the need for optimized residence time to maximize product purity and conversion efficiency before feeding the overhead into the pressure swing column.

Figure 5, the ethanol conversion versus residence time profile, provided critical insight into the dynamic behavior of the esterification reaction within the reactive distillation column. Initially, a rapid increase in conversion was observed, with approximately 52.1% conversion achieved within the first 10 minutes. This rapid rate was attributed to the high concentration of reactants and efficient mass transfer within the reactive trays. As time progressed, the rate of conversion began to decline, with conversion reaching 77.9% at 20 minutes and gradually approaching a plateau of 83.5% by the 35th minute. The plateau signified the system's approach to chemical equilibrium, beyond which additional residence time did not significantly enhance conversion. This behavior underscored the effectiveness of the column design in achieving high conversion within a relatively short operational period. From a process optimization standpoint, these findings suggested that 30 to 35 minutes of residence time was sufficient for a near-complete reaction, balancing productivity with energy and equipment efficiency.

The impact of pressure swing distillation on separating the azeotropic mixture formed in the high-pressure reactive distillation column is illustrated in Figure 6 through the concentration profiles of ethyl acetate and ethanol across the stages of the Low-Pressure Column (LPC). The highest concentration of ethyl acetate was observed at the top of the LPC, attributed to its lower boiling point at reduced pressure. As the components descended the column, ethyl acetate content decreased from 0.74 mole to 0.48 mole while ethanol mole fraction increased from 0.26 mole to 0.52 mole, showing effective separation. Ethanol accumulated toward the column base, indicating successful disruption of the azeotrope due to pressure reduction. This pressure-sensitive azeotrope responded well to the PSD strategy by allowing component volatility shifts at 0.5 bar, a condition under which ethyl acetate more readily vaporized while ethanol preferred the liquid phase. The uniform gradient observed in the profile confirmed good stage efficiency and mass transfer between phases. Additionally, the steady trend suggested minimal entrainment or channelling within the column. These results validated the feasibility of PSD for azeotrope elimination in ethyl acetate–ethanol systems. Leveraging the differences in component volatility under reduced pressure enabled the recovery of high-purity ethyl acetate at the column top, while ethanol was recycled. This highlights the importance of tray arrangement and pressure settings in effectively separating azeotropic mixtures.

Figure 7 analyzed the influence of operating pressure on the mole fractions of ethanol and ethyl acetate, with a focus on azeotropic behavior. The results revealed that the ethanol–ethyl acetate azeotrope is sensitive to pressure variations. At reduced pressures, a higher mole fraction of ethyl acetate and a lower mole fraction of ethanol were observed, indicating improved separation. Conversely, as the pressure increased, ethyl acetate concentrations declined while ethanol concentrations rose, signifying the emergence of an azeotrope that hindered effective separation. At around 12 bar, the azeotropic composition was observed, where ethanol and ethyl acetate co-boiled, making further separation by simple distillation ineffective.

This reinforced the necessity of using Pressure Swing Distillation (PSD) as an effective technique to overcome the azeotrope. Operating the high-pressure column at 12 bar allowed the azeotropic mixture to form, which was then fed into the low-pressure column operating at 0.5 bar, where the azeotrope was broken due to the shift in equilibrium composition. This graph supported the design strategy of using dual columns with differing pressures for efficient separation. It also highlighted that careful control of pressure was essential to maximize ethyl acetate purity and minimize ethanol content in the final product, reinforcing PSD as a robust method in process intensification.

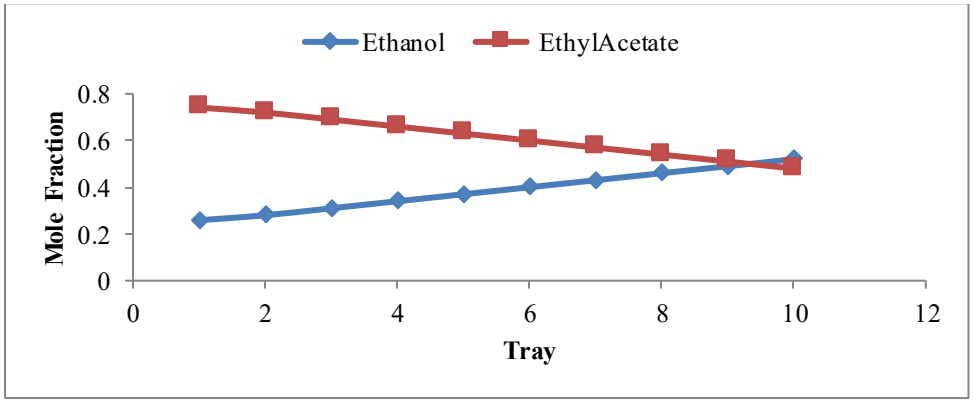

Fig. 6 Ethyl Acetate and Ethanol Mole Fraction along LPC Trays

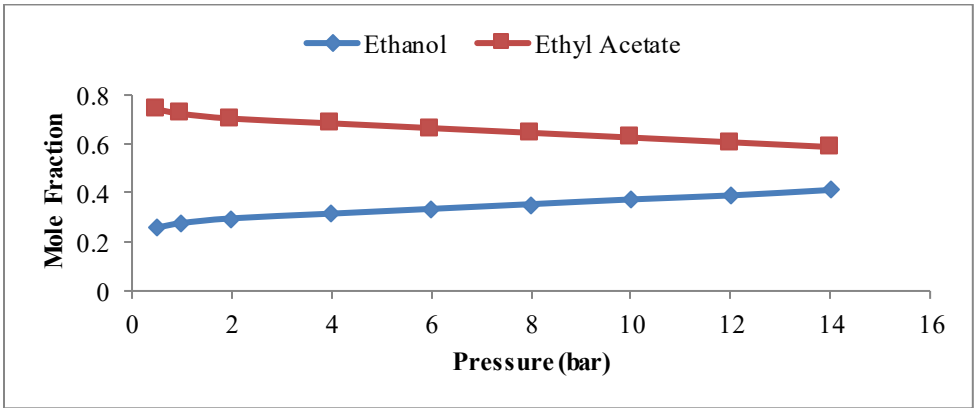

Fig. 7 Azeotropic Composition Vs Column Pressure

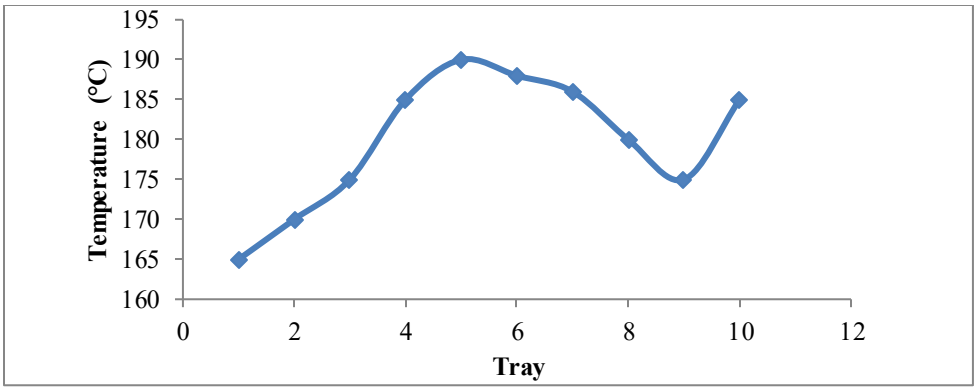

Fig. 8 Temperature Progression along the Reactive Distillation Column (RDC)

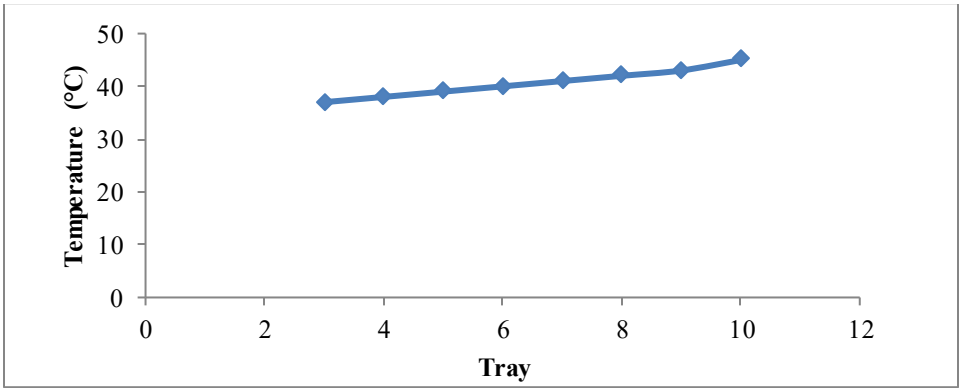

Fig. 9 Temperature Variation along the Low-Pressure Column (LPC)

Figure 8 presents the temperature gradient throughout the trays of the reactive distillation column, reflecting the thermal conditions essential for facilitating the esterification between ethanol and acetic acid. A consistent rise in temperature was observed from the top condenser down to the bottom reboiler. The section designated for reaction between trays 4 and 7 reached its maximum temperature of 190°C on tray 5, primarily due to the heat generated by the exothermic nature of the esterification process. The upper stages remained cooler, favoring condensation and product recovery, while the lower trays facilitated the stripping of heavy components.

The reboiler maintained a temperature of 185°C, ensuring vaporization and circulation of reactants and products. This gradient promoted both effective separation and reaction by maintaining temperature zones tailored to each function. The steady progression implied efficient heat integration within the column and confirmed that energy from the exothermic reaction was effectively utilized to support vapour-liquid equilibrium. The well-structured temperature distribution enhanced component volatility control and optimized the reaction efficiency. Overall, the temperature profile validated the placement of the trays and confirmed that the column design effectively enabled both reaction and separation to occur simultaneously, showcasing process intensification within a thermally optimized reactive distillation system.

Figure 9 displays the temperature distribution across the Low-Pressure Column (LPC) trays operated at 0.5 bar to disrupt the azeotropic mixture of ethanol and ethyl acetate. Temperatures ranged from 35°C at the overhead to 45°C at the column base, reflecting a gentle and uniform thermal gradient. This steady temperature increase suggested efficient heat transfer and maintained phase stability throughout the column.

Operating under reduced pressure lowered the boiling points of both components, promoting the preferential vaporization of ethyl acetate at the top while allowing ethanol to condense and collect at the Bottom. The temperature gradient confirmed that ethyl acetate, having a lower boiling point, was effectively stripped and directed to the distillate stream, while ethanol concentrated toward the reboiler. The stable progression with no temperature spikes or irregularities suggested excellent tray efficiency and thermal control.

The profile also reflected good hydraulic performance, as there was no indication of flooding or weeping. The temperature behavior confirmed that the LPC complemented the high-pressure column by finalizing the separation process and ensuring azeotrope disruption. Thus, operating at low pressure with mild thermal input, the LPC design played a crucial role in maximizing ethyl acetate recovery and improving overall process energy efficiency.

4. Conclusion

In this research, mathematical models were effectively formulated for six sections of the distillation column—namely, the reflux drum, rectifying section, reactive zone, feed stage, stripping section, and column base—to simulate the esterification process between ethanol and acetic acid for ethyl acetate production within a Reactive Distillation Column (RDC). Using ASPEN PLUS, the High-Pressure Column (HPC) at 12 bar and 78 maximized reaction conversion, producing ethyl acetate and water, while the low-pressure column (LPC) at 0.5 bar and 40 effectively eliminated the ethyl acetate-ethanol azeotrope through Pressure Swing Distillation (PSD). MATLAB simulations closely corroborated ASPEN PLUS results, yielding ethyl acetate mole fractions of 0.7411 and 0.7200, respectively, with ethanol at 0.2589 and 0.2800. Validation against literature data showed deviations of 13.74% for ethanol and -4.57% for ethyl acetate, confirming model accuracy. Optimal feed stage placement (stage 3 for ethanol, stage 2 for acetic acid) enhanced product purity. The 10-stage column design provided finer resolution, improving separation efficiency. The outcomes support process intensification strategies by providing a validated and scalable pathway for producing high-purity ethyl acetate.

Acknowledgement

Engr. Yiga Francis is credited with initiating the research concept and gratefully acknowledges Engr's insightful contributions. Okwu Kingsley Chidiebere in shaping and organizing the research plan. The authors sincerely thank the Department of Chemical/Petrochemical Engineering, Rivers State University, for providing steadfast academic and technical assistance throughout the project. Special appreciation is also extended to Professor K.K. Dagde and Professor J.G. Akpa for their dedicated supervision and valuable academic mentorship during the course of this research.

Nomenclature

Symbol	Meaning	Unit
B	Bottom flow rate	mol/hr
C_p	Specific heat capacity at constant pressure	J/mol-^oC
C_i	The molar concentration of species i	mol/ m^3
C_T	The total concentration of the bulk mixture	mol/ m^3
D	Distillate flow rate	mol/hr
F	Feed flow rate	mol/hr
h_{Fj}	Specific enthalpy of feed to the jth tray	J/mol
h_j	Specific enthalpy of vapor/liquid on jth tray	J/mol
h_{j+1}	Specific enthalpy of liquid from (j+1)th tray	J/mol
h_{j-1}	Specific enthalpy of vapor from (j-1)th tray	J/mol
$-\Delta H_R$	Heat of reaction	J/mol
I	Species/Component	
J	Representative tray	
K	Distribution coefficient	
k_1	The rate constant of the forward reaction	m^3/ mol-hr
k_2	The rate constant of the backwards reaction	m^3/ mol-hr
L_j	Liquid flow rate on the jth tray	mol/hr
L_{j-1}	Liquid flow rate on (j-1)th tray	mol/hr
L_{j+1}	Liquid flow rate on (j+1)th tray	mol/hr
M_j	Molar hold up on the JTH tray	mol
N	Total number of components/species	
Nt	Total number of trays	
Q_{Cond}	Condenser heat duty	J/hr
Q_{Reb}	Reboiler heat duty	J/hr
$r_{j,i}$	Rate of reaction of species i on the jth tray	mol/hr
T_j	Temperature of jth tay	^oC
T_{j-1}	Temperature of(j-1)th tray	^oC
T_{j+1}	Temperature of (j+1)th tray	^oC
V_j	The vapor flow rate on the jth tray	mol/hr

V_{j-1}	The vapor flow rate from the (j-1)th tray	mol/hr
V_{j+1}	the vapor flow rate from the (j+1)th tray	mol/hr
V_{Rj}	The liquid volume on tray j	m^3
$x_{B,i}$	The Bottom's composition of species i	
$x_{D,i}$	Distillate composition of species i	
$x_{j,i}$	The liquid composition of species i on the jth tray	
$x_{j-1,i}$	The liquid composition of species i on the (j-1)th tray	
$x_{j+1,i}$	The liquid composition of species i on the (j+1)th tray	
$y_{j,i}$	The vapour composition of species i on the jth tray	
$y_{j-1,i}$	The vapor composition of species i on the (j-1)th tray	
$y_{j+1,i}$	The vapor composition of species i on the (j-1)th tray	
$z_{j,i}$	The feed composition of species i	

References

[1] Damandeep Singh, Raj Kumar Gupta, and Vineet Kumar, "Simulation Studies on Homogenously Catalyzed Finishing Reactive Distillation for Ethyl Acetate Production," *Chemical Engineering Communications*, vol. 207, no. 1, pp. 1-14, 2019. [CrossRef] [Google Scholar] [Publisher Link]

[2] N. Calvar, B. Gómez, and A. Domínguez, "Esterification of Acetic Acid with Ethanol: Reaction Kinetics and Operation in a Packed Bed Reactive Distillation Column," *Chemical Engineering and Processing: Process Intensification*, vol. 46, no. 12, pp. 1317-1323, 2007. [CrossRef] [Google Scholar] [Publisher Link]

[3] Chunli Li et al., "Process Intensification and Energy Saving of Reactive Distillation for Production of Ester Compounds," *Chinese Journal of Chemical Engineering,* vol. 27, no. 6, pp. 1307-1323, 2019. [CrossRef] [Google Scholar] [Publisher Link]

[4] J. Gmehling, U. Onken, and Wolfgang Arlt, *Vapor-Liquid Equilibrium Data Collection*, Dechema, pp. 1-600, 1997. [Google Scholar] [Publisher Link]

[5] Yadollah Tavan, and Seyyed Hossein Hosseini, "Design and Simulation of a Reactive Distillation Process to Produce High-Purity Ethyl Acetate," *Chemical Engineering Research and Design*, vol. 44, no. 4, pp. 577-585, 2013. [CrossRef] [Google Scholar] [Publisher Link]

[6] Miguel A. Santaella, Alvaro Orjuela, and Paulo C. Narváez, "Comparison of Different Reactive Distillation Schemes for Ethyl Acetate Production using Sustainability Indicators," *Chemical Engineering and Processing: Process Intensification*, vol. 96, pp. 1-13, 2015. [CrossRef] [Google Scholar] [Publisher Link]

[7] K.K.C.W. Kandanapitiya, and M.Y. Gunasekera, "Modelling of Reactive Distillation for Acetic Acid Esterification," *Engineer: Journal of the Institution of Engineers, Sri Lanka*, vol. 48, no. 4, pp. 17-23, 2015. [CrossRef] [Google Scholar] [Publisher Link]

[8] Jing Yang et al., "Simulation of Pressure-swing Distillation for Separation of Ethyl Acetate-Ethanol-Water," *IOP Conference Series: Materials Science and Engineering: 1st International Conference on Frontiers of Materials Synthesis and Processing*, Changsha, China, vol. 274, pp. 1-8, 2017. [CrossRef] [Google Scholar] [Publisher Link]

[9] Liu Shuhan et al., "Design and Control of Ethyl Acetate–Ethanol Separation via Pressure Swing Distillation," *Theoretical Foundations of Chemical Engineering*, vol. 57, pp. 917-932, 2023. [CrossRef] [Google Scholar] [Publisher Link]

[10] Sohail Rasool Lone, and Syed Akhlaq Ahmad, "Modeling and Simulation of Ethyl Acetate Reactive Distillation Column using Aspen Plus," *International Journal of Scientific & Engineering Research*, vol. 3, no. 8, pp. 1-5, 2012. [Google Scholar]

[11] Adnan Aldemir, Dilan Ersingün, and İsmail Bayram, "Dynamic Simulation of a Reactive Distillation Column for Ethyl Acetate Production: Optimization of Operating Conditions Using Response Surface Methodology," *Yuzuncu Yil University Journal of the Institute of Natural and Applied Sciences*, vol. 27, no. 2, pp. 365-379, 2022. [CrossRef] [Google Scholar] [Publisher Link]

[12] Xiuhui Huang et al., "Thermodynamic Analysis and Process Simulation of an Industrial Acetic Acid Dehydration System via Heterogeneous Azeotropic Distillation," *Industrial & Engineering Chemistry Research*, vol. 52, no. 8, pp. 2944-2957, 2013. [CrossRef] [Google Scholar] [Publisher Link]

[13] Statista, Number of Power Conditioners for Stationary on-grid Energy Storage Systems Shipped in Japan in Fiscal Year 2022, by Type. [Online]. Available: https://www.statista.com/statistics/1298183/ethyl-acetate-market-size-worldwide/

[14] Natalie J. Czarnecki, Scott A. Owens, and R. Bruce Eldridge, "Extractive Dividing Wall Column for Separating Azeotropic Systems: A Review," *Industrial & Engineering Chemistry Research*, vol. 62, no. 14, pp. 5750-5770, 2023. [CrossRef] [Google Scholar] [Publisher Link]

[15] Matthias Wierschem, and Andrzej Górak, *Reactive Distillation*, Reference Module in Chemistry, Molecular Sciences and Chemical Engineering, Elsevier, 2018. [CrossRef] [Google Scholar] [Publisher Link]

[16] Shoutao Ma et al., "Energy-Saving Thermally Coupled Ternary Extractive Distillation Process using Ionic Liquids as Entrainer for Separating Ethyl Acetate-Ethanol-Water Ternary Mixture," *Separation and Purification Technology*, vol. 226, pp. 337-349, 2019. [CrossRef] [Google Scholar] [Publisher Link]

[17] Andras Jozsef Toth, "Comprehensive Evaluation and Comparison of Advanced Separation Methods on the Separation of Ethyl Acetate-Ethanol-Water Highly Non-Ideal Mixture," *Separation and Purification Technology*, vol. 224, pp. 490-508, 2019. [CrossRef] [Google Scholar] [Publisher Link]

[18] Dong L. Zhang et al., "Separation of Ethyl Acetate−Ethanol Azeotropic Mixture Using Hydrophilic Ionic Liquids," *Industrial & Engineering Chemistry Research*, vol. 47, no. 6, pp. 1995-2001, 2008. [CrossRef] [Google Scholar] [Publisher Link]